LANGMUIR

Article

pubs.acs.org/Langmuir

Differential Interaction of Synthetic Glycolipids with Biomimetic Plasma Membrane Lipids Correlates with the Plant Biological Response

Mehmet Nail Nasir,[*,†] Laurence Lins,[†] Jean-Marc Crowet,[†] Marc Ongena,[‡] Stephan Dorey,[§] Sandrine Dhondt-Cordelier,[§] Christophe Clément,[§] Sandrine Bouquillon,[∥] Arnaud Haudrechy,[∥] Catherine Sarazin,[⊥] Marie-Laure Fauconnier,[#] Katherine Nott,[#] and Magali Deleu[*,†]

[†]Laboratoire de Biophysique Moléculaire aux Interfaces, Structure Fédérative de Recherche Condorcet, Gembloux Agro-Bio Tech, [‡]Microbial Processes and Interactions Laboratory (MiPI), Structure Fédérative de Recherche Condorcet, Gembloux Agro-Bio Tech, and [#]Laboratoire de Chimie Générale et Organique, Structure Fédérative de Recherche Condorcet, Gembloux Agro-Bio Tech, Université de Liège, 2 Passage des Déportés, B-5030 Gembloux, Belgique

[§]Reims Champagne-Ardenne University, URVVC-SE-EA 2069, Stress, Defense and Plant Reproduction Laboratory, Structure Fédérative de Recherche Condorcet Fédération de Recherche, Centre National de la Recherche Scientifique, 3417BP 1039, F-51687 Reims Cedex 2, France

[∥]Institut de Chimie Moléculaire de Reims, UMR CNRS 7312, Structure Fédérative de Recherche Condorcet, UFR Sciences, BP 1039, F-51687 Reims Cedex 2, France

[⊥]Unité de Génie Enzymatique et Cellulaire, FRE CNRS 3580, Structure Fédérative de Recherche Condorcet, Université de Picardie Jules Verne, 33 Rue Saint-Leu, F-80039 Amiens, France

Supporting Information

ABSTRACT: Natural and synthetic amphiphilic molecules including lipopeptides, lipopolysaccharides, and glycolipids are able to induce defense mechanisms in plants. In the present work, the perception of two synthetic C14 rhamnolipids, namely, Alk-RL and Ac-RL, differing only at the level of the lipid tail terminal group have been investigated using biological and biophysical approaches. We showed that Alk-RL induces a stronger early signaling response in tobacco cell suspensions than does Ac-RL. The interactions of both synthetic RLs with simplified biomimetic membranes were further analyzed using experimental and in silico approaches. Our results indicate that the interactions of Alk-RL and Ac-RL with lipids were different in terms of insertion and molecular responses and were dependent on the lipid composition of model membranes. A more favorable insertion of Alk-RL than Ac-RL into lipid membranes is observed. Alk-RL forms more stable molecular assemblies than Ac-RL with phospholipids and sterols. At the molecular level, the presence of sterols tends to increase the RLs' interaction with lipid bilayers, with a fluidizing effect on the alkyl chains. Taken together, our findings suggest that the perception of these synthetic RLs at the membrane level could be related to a lipid-driven process depending on the organization of the membrane and the orientation of the RLs within the membrane and is correlated with the induction of early signaling responses in tobacco cells.

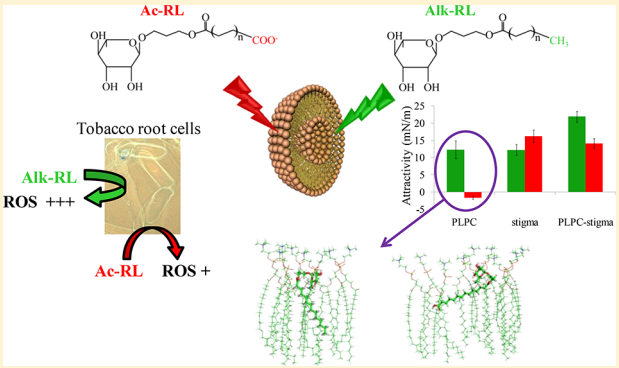

INTRODUCTION

Biosurfactants are promising molecules because of their potential applications in several fields (industry, agronomy, and the environment). They are highly biodegradable and biocompatible and present a low toxicity.[1] Among them, amphiphilic molecules from natural and synthetic origins have been distinguished by their potential interesting biological properties, especially for plant protection.[2−6] For instance, natural lipopeptides, lipopolysaccharides (LPS), rhamnolipids (RLs), and synthetic glycolipids are able to stimulate plant defense responses.[3,7−9] The mechanism involved in the perception of amphiphilic molecules by the plant cell surface is far from being known. LPS recognition involves receptor-like kinases, but the surfactin lipopeptide perception seems to involve a lipid-driven process at the plasma membrane level.[10,11] It has been suggested that surfactin insertion into the plasma membrane could disturb the lipid compartmentalization or induce curvature constraints in the cell membranes.

Received: April 19, 2017
Revised: July 19, 2017
Published: July 27, 2017

DOI: 10.1021/acs.langmuir.7b01264
Langmuir 2017, 33, 9979−9987

In this way, it could lead to direct activation of mechanosensitive channels or proteins involved in signaling that in turn activate a biochemical cascade of molecular events leading to the establishment of defensive responses.[11] It has also been demonstrated that a linear fatty acid chain with 14 carbons (surfactin nC14) is necessary for the biological activity of surfactin.[11] Natural RLs of *Pseudomonas aeruginosa* are amphiphilic compounds made of one or two rhamnose units (linked by a 1,2-glycosidic bond) that constitute the polar headgroup that is connected to one or two hydroxy fatty acids linked to each other by an ester bond, which make up the hydrophobic tail.[1,3] These compounds have biotechnological applications related to environmental concerns, such as the bioremediation of hydrocarbons, organic pollutants, and heavy-metal-contaminated sites.[12−14] They are also used in the production of fine chemicals and surface coatings as well as additives for food and cosmetics and as potent inducers of plant defense responses.[15−18] To generate new biologically active compounds for plant defense, we synthesized hybrid glycolipids with a rhamnose headgroup and a single fatty acid chain. To obtain strong biological activity similar to that of amphiphilic molecule surfactin produced by *B. amyloliquefaciens* S499,[11] we selected congeners with a linear chain comprising 14 carbons. The synthetic RLs used in our study differ only at the level of the terminal group; Alk-RL has a $-CH_3$ group whereas Ac-RL has a carboxylic acid group at the end of the carbon chain (Figure 1). Ac-RL was inspired from the carboxylic acid function present in natural RLs, whereas Alk-RL mimics the surfactin fatty acid chain.

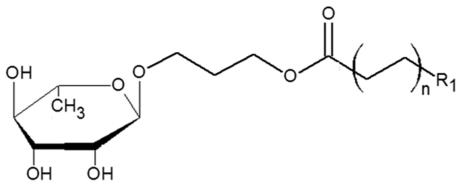

Figure 1. General structure of synthetic Alk-RL (R1 = $-CH_3$) and Ac-RL (R1= $-COOH$) with $n = 6$.

Plants produce reactive oxygen species (ROS) within minutes in response to microbial-associated molecular patterns.[19−21] In addition to their role as antimicrobial agents targeting pathogens, ROS are important in cell signaling to stimulate defense gene expression.[22,23] The generation of ROS by plant cells, called "oxidative burst", is a signaling marker related to biotic and abiotic stresses[24] and is often linked to the perception of exogenous stresses by the plant.[11] In this work, we have first demonstrated that synthetic Alk-RL and Ac-RL are able to trigger the production of ROS by cultured tobacco cells, suggesting that these compounds are perceived by plant cells. Because synthetic RLs have a global amphiphilic structure that is similar to that of surfactin, we hypothesized that the interaction of the molecules with the lipid fraction of the plant plasma membrane (PPM) is involved in the process. To investigate the perception of synthetic RLs at the membrane level, the interactions of Alk-RL and Ac-RL with PPM were analyzed using experimental and in silico approaches on simplified biomimetic membranes composed of palmitoyl-linoleoyl-phosphatidylcholine (PLPC) and/or stigmasterol, which are representative of phospholipids and sterols, respectively, found in the PPM.[25,26] The results obtained with the biophysical approach strongly correlate with the induction of the signaling response in plants, suggesting a link between the interactions of synthetic RLs with PPM lipids and one of their biological activities.

MATERIALS AND METHODS

Materials. Synthetic RLs Alk-RL and Ac-RL were synthesized in our laboratories as described in our previous work.[1] Briefly, they were enzymatically generated by the introduction of a primary alcohol function onto rhamnose by the glycosylation of propane-1,3-diol catalyzed by a glycosidase, followed by a lipase-catalyzed esterification step of the hydroxyl group with a mono- or dicarboxylic fatty acid. Their purity was checked by high-performance liquid chromatography and was superior to 99%. A natural RL mixture from *Pseudomonas aeruginosa* was purchased from Jeneil Biotech, with a mono-RL/di-RL ratio of 65/35. Surfactin was produced and purified as previously described.[27] Its purity (>95%) was ascertained by high-performance liquid chromatography. We purchased 1-palmitoyl-2-linoleoyl-*sn*-glycero-3-phosphocholine (PLPC) and stigmasterol from Avanti Polar Lipids and used them without further purification. Deuterium oxide (D_2O) at 99.9% isotopic purity and dimethyl sulfoxide (DMSO) were provided from Sigma Chemical Co. The ultrapure water was produced by a Millipore system available in our laboratory, and the resistivity was 18.2 MΩ cm. Chloroform and methanol were purchased from Scharlau.

Oxidative Burst Assays with Tobacco Cells. Tobacco suspension cells (*Nicotiana tabacum* L. cv. bright yellow-2) were cultivated as described previously.[11] A method based on a chemiluminescence measurement was used to monitor the production of extracellular ROS. Indeed, hydrogen peroxide from the ferricyanide-catalyzed oxidation of luminol was measured using a luminometer (TD-20/20 Luminometer, Turner Designs, Fresno, CA, USA). After treatment with Alk-RL or Ac-RL (1 mM stock solution in DMSO), a 50 μL aliquot of the cell suspension (final concentration 0.15 g fresh weight·mL^{-1}) was added to 100 μL of 50 mM phosphate buffer (pH 7.9) and 100 μL of 1.1 mM luminol in phosphate buffer. The reaction was started by the addition of 100 μL of freshly prepared 14 mM $K_3[Fe(CN)_6]$, and the signal was integrated over the first 30 s after the reaction began. Control experiments were performed with natural RLs (positive control) and with DMSO (negative control).

Adsorption Experiments at Constant Surface Area. Adsorption experiments were performed in a KSV Minitrough (Helsinki, Finland, 7.5 × 20 cm^2). The subphase was ultrapure water (~80 mL) with a constant temperature at 22.0 ± 1.0 °C. The subphase was continuously stirred with a magnetic stirrer. Pure PLPC, pure stigmasterol molecules or their mixture (70/30 molar ratio) in chloroform/methanol (2/1 v/v) solvent, was spread at the air−water interface to reach the desired initial surface pressure. After 20 min of waiting for solvent evaporation and film stabilization, Alk-RL or Ac-RL in DMSO solution was injected underneath the preformed lipid monolayer. The final subphase concentration was 1 μM for Alk-RL and 10 μM for Ac-RL. Their adsorption to the lipid monolayers was followed by an increase in surface pressure. As a control experiment, the same volume of pure DMSO was injected underneath the lipid monolayer, and no change in the surface pressure was observed. The uncertainties in the maximum insertion pressure (MIP) and the $\Delta\Pi_0$ were calculated as described previously.[26,28,29] Given that Alk-RL and Ac-RL do not have the same concentration within the subphase, the differential Π_0 ($d\Pi_0$) parameter was defined to compare them. It was calculated as follows

$$d\Pi 0 = \Delta\Pi_0 - \Pi_e$$

where $\Delta\Pi_0$ corresponds to the y intercept of the linear regression of the $\Delta\Pi$ vs Π_i plot and Π_e is the surface pressure increase at the equilibrium obtained in an independent experiment performed at the same synthetic RL concentration but without lipids spread at the interface.

Preparation of Multilamellar Vesicles (MLVs). MLVs were prepared from pure PLPC or PLPC/stigmasterol (70/30 molar ratio). Lipids were dissolved in a chloroform/methanol mixture (2/1 v/v)

DOI: 10.1021/acs.langmuir.7b01264
Langmuir 2017, 33, 9979−9987

alone or in the presence of Alk-RL or Ac-RL at a molar ratio of lipid/RL of 10/1. The chloroform/methanol mixture was evaporated to obtain a lipid film before drying it under vacuum overnight. The resulting film was hydrated by deuterium oxide above the phase-transition temperature of lipids. The hydrated film was vortex mixed continuously to obtain MLV.

Infrared Spectroscopy (FTIR). Infrared spectra were recorded by means of a Bruker Equinox 55 spectrometer (Karlsruhe, Germany) equipped with a liquid-nitrogen-cooled DTGS detector. The number of scans was 128 at 4 cm^{-1} resolution. During all measurements, the spectrometer was continuously purged with a flux of N_2. All of the experiments were performed with a demountable cell (Bruker) equipped with CaF_2 windows. Each spectrum is representative of at least three independent measurements.

In Silico Methods. The interactions of Alk-RL or Ac-RL with model membranes were analyzed by molecular modeling. The 3D structures of Alk-RL, Ac-RL, PLPC, and stigmasterol were constructed using HyperChem software (Hypercube, Inc.). The molecular geometry was optimized with the steepest-descent method using the MM+ force field, and a systematic analysis of the torsion angles using the structure tree method was performed as described previously.[30] The most probable structure corresponding to the lowest conformational energy was used for further calculations. The insertion of the molecule within an implicit bilayer was computed by the IMPALA procedure as described in Ducarme et al.,[31] and the interaction energies in a lipid monolayer (PLPC or stigmasterol) were calculated using the Hypermatrix procedure.

Briefly, in the IMPALA method, an implicit membrane is described as a continuous medium whose properties vary along the axis perpendicular to the bilayer plane (z axis). The membrane properties are represented by energy restraints.[31] The synthetic RL molecule is systematically moved along the z axis by 1 Å steps, and the restraints are calculated for each position. A profile of the energy restraints as a function of the penetration into the implicit bilayer is obtained.

The simple docking method called Hypermatrix is described in detail elsewhere.[26] Briefly, the synthetic RL molecule is put in a fixed position at the center of the system and oriented at the hydrophobic/hydrophilic interface, while the lipid molecule, also oriented at the lipid/water interface, is positioned around the molecule by rotations and translations (more than 10^7 positions tested). For each position, an energy value is calculated according to a home-designed force field.[32] The energy values together with the coordinates of all assemblies are stored in a matrix and classified according to decreasing values. The first stable matching is used to decide the position of the first lipid. The position of the second lipid is then defined as the next most energetically favorable orientation stored in the matrix, taking steric and energetic constraints due to the presence of the first lipid molecule into account. The process is completed when the central molecule is completely surrounded with lipids.[26]

RESULTS

Synthetic RLs Are Able to Induce Oxidative Burst in Plant Cells. Luminol-based chemiluminescence assays were used to monitor the induction of extracellular hydrogen peroxide (representative of ROS) production by tobacco suspension cells upon treatment with Alk-RL or Ac-RL in comparison to a natural RL mixture consisting of mono- and di-RL and surfactin, taken as positive controls of defense inducers. Figure 2 shows the production of hydrogen peroxide compared to a basal response by plant cells.

Alk-RL and Ac-RL clearly induced an oxidative burst, which was higher than the negative control and of the same order of magnitude as the natural RL mixture for Alk-RL (Figure 2A). Interestingly, the oxidative burst with these compounds is lower than after the surfactin challenge.

ROS production appears to be concentration-dependent (Figure 2B). For each concentration tested, ROS production in the presence of Alk-RL is significantly higher than for Ac-RL.

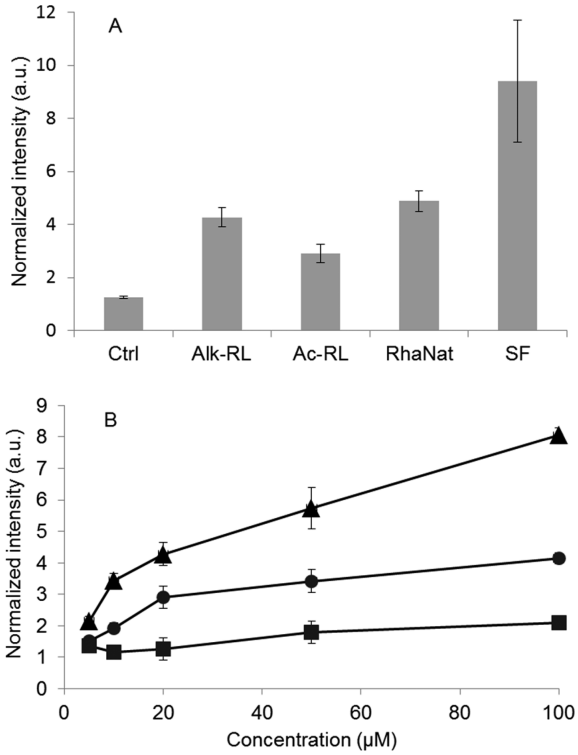

Figure 2. (A) Induction of extracellular hydrogen peroxide production by tobacco cells measured by chemiluminescence in response to different molecules at 20 μM. Surfactin (SF) and natural rhamnolipids (RhaNat) are used as positive controls, and Ctrl consists of DMSO used as a negative control. (B) Concentration-dependent extracellular hydrogen peroxide production by tobacco cells. Squares, Ctrl (DMSO); triangles, Alk-RL; and circles, Ac-RL.

Moreover, the concentration effect is more pronounced with Alk-RL than with Ac-RL. At higher concentrations (100 μM), ROS production in response to Alk-RL is approximately 8 times higher than for the control, whereas it is only 2 times higher for Ac-RL. It is worth noting that no cell death was observed, even at the highest concentration tested (100 μM, Figure S1).

The Adsorption of Synthetic RLs to Different Model Membranes Depends on Their Chemical Structure and on the Membrane Composition. Prior to this step, preliminary experiments were performed to determine the critical aggregation concentration (CAC) of both molecules (Figure S2). The CACs of Alk-RL and Ac-RL are 1.9 ± 1.0 and 11.2 ± 2.5 μM, respectively. For adsorption assays, a concentration slightly below but close to the CAC and high enough to observe a significant increase in surface pressure was chosen for each molecule: concentrations of 1 and 10 μM were chosen for Alk-RL and Ac-RL, respectively. No significant adsorption was observed with Ac-RL at 1 μM (data not shown).

To test the possible interaction of the synthetic RLs with PPM, we used lipid Langmuir monolayers mimicking the external leaflet of PPM. Reconstituted monolayers made of pure PLPC, pure stigmasterol, or a PLPC/stigmasterol mixture (70/30 molar ratio) were used as models of the plant plasma membrane. Adsorption of Alk-RL or Ac-RL to these different lipid monolayers was followed by surface pressure measurements over time.[28] Figure 3 shows a typical plot of the maximal surface pressure variation ($\Delta\Pi$) due to the Alk-RL or Ac-RL

DOI: 10.1021/acs.langmuir.7b01264
Langmuir 2017, 33, 9979−9987

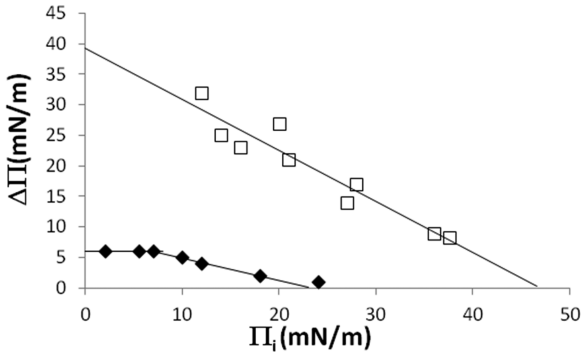

Figure 3. Adsorption of Alk-RL (white square) or Ac-RL (black diamond) to preformed PLPC monolayers at the defined initial surface pressure (Π_i). Influence of Π_i on the maximal variation of the surface pressure ($\Delta\Pi$). Each point was obtained by an independent experiment.

adsorption versus the initial surface pressure of the PLPC monolayer (Π_i). For Alk-RL, $\Delta\Pi$ decreases linearly with increasing values of Π_i, indicating that a greater initial surface pressure related to a higher density of PLPC molecules at the air−water interface leads to a weaker adsorption of the Alk-RL to the monolayer. The reduction of the free space with increasing Π_i values can explain this observation. For Ac-RL, biphasic behavior is observed, as already reported by Hädicke and Blume for small peptides.[33] It could be explained by an overlay of two processes, the Ac-RL incorporation into the monolayer and a lipid condensation. This behavior is observed only with PLPC monolayer and not with stigmasterol or PLPC/stigmasterol monolayers.

From this curve, the maximal insertion pressure (MIP) is determined at the intersection of the linear regression with the x axis as described previously[26,29] and presented in Figure 4. The MIP corresponds to the surface pressure beyond which no adsorption can occur and provides information about the insertion power of the molecule into a lipid membrane.

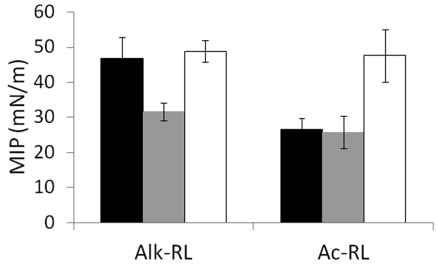

Figure 4. Maximal insertion pressure (MIP) of Alk-RL and Ac-RL for different lipid monolayers consisting of PLPC (black), stigmasterol (gray), or PLPC-stigmasterol (white). The MIP was obtained by a linear regression of the $\Delta\Pi = f(\Pi_i)$ plot with the x axis.

MIPs of Alk-RL for PLPC, stigmasterol, and PLPC/stigmasterol monolayers were 46.8 ± 6, 31.6 ± 2.6, and 48.9 ± 3.1 mN/m, respectively (Figure 4). Those values are greater than 30 mN/m, which is a postulated value for the lateral pressure prevailing in natural biological membranes.[34] Even if the lipid composition of biological membranes is more complex, a MIP value higher than 30 mN/m is interpreted as a favorable insertion of the tested molecule within biological membranes.[34] Hence, it can be suggested that Alk-RL is able to insert readily within biological membranes. For Ac-RL, the MIP values for PLPC, stigmasterol, and PLPC/stigmasterol monolayers were 26.6 ± 3.2, 25.8 ± 4.7, and 47.6 ± 7.5 mN/m, respectively. In pure lipid monolayers, the insertion of Ac-RL is less favorable than that of Alk-RL, whereas in PLPC/stigmasterol mixed monolayers the insertion of Ac-RL is similar to that of Alk-RL.

Another parameter, the differential Π_0 ($d\Pi_0$), reflecting the attractive effect of the lipids at null surface pressure was also calculated (Figure 5). A positive value of $d\Pi_0$ suggests an

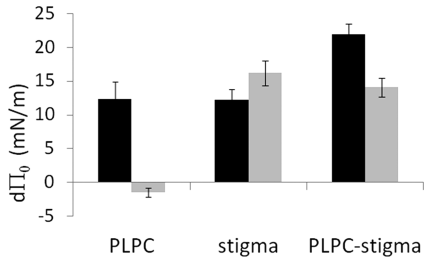

Figure 5. Differential Π_0 ($d\Pi_0$) is calculated for Alk-RL (black bars) and Ac-RL (gray bars) in the presence of different monolayers: PLPC, stigmasterol (stigma), and PLPC-stigmasterol.

attractive effect of the lipids on molecule adsorption, and a negative value indicates instead an unfavorable impact of the lipids on molecule insertion into the monolayer.

For the PLPC monolayer, the $d\Pi_0$ values for Alk-RL and Ac-RL are positive and close to zero, respectively, suggesting that the insertion of Alk-RL but not Ac-RL is favored by the presence of PLPC. This result is in agreement with the adsorption kinetics (slope of the curve) of synthetic RLs to PLPC monolayers at a similar initial surface pressure (Figure S3). Even though Ac-RL was more concentrated than Alk-RL within the subphase, its adsorption speed to PLPC monolayers was lower (Figure S3). For the stigmasterol monolayer, the $d\Pi_0$ of Ac-RL is slightly higher than that of Alk-RL. For the mixed PLPC/stigmasterol monolayer, the $d\Pi_0$ of Alk-RL is significantly higher than that of Ac-RL, but in this case, the mixed lipids also exert an attractive effect on Ac-RL.

Following the monolayer studies, the insertion capacity of synthetic RLs through a lipid bilayer was analyzed. Their insertion was simulated through an implicit membrane by the IMPALA procedure. A plot showing the energy restraint values as a function of the insertion depth of the molecule mass center (Figure 6) indicates that the most favorable position of the molecules is near the lipid hydrophobic tail/polar head interface of either bilayer sheet. The minimal restraint value is significantly lower for Alk-RL than for Ac-RL, suggesting a more energetically favorable insertion of Alk-RL into the bilayer. In the hydrocarbon core of the membrane, the molecules also exhibit different behavior. For Alk-RL, the restraint value is close to zero, whereas for Ac-RL, it becomes positive, predicting that this last molecule should not be stable when positioned near the hydrophobic core of the bilayer.

The Interaction of Synthetic RLs with Membrane Lipids Involves Both the Hydrophilic and Hydrophobic Parts of Lipids. Multilamellar vesicles (MLVs) composed of PLPC or PLPC/stigmasterol (70/30 molar ratio) were prepared in the absence or in the presence of synthetic RLs. The FTIR spectra of MLVs were recorded to analyze the interactions between the synthetic RLs and the lipids at the molecular level.

DOI: 10.1021/acs.langmuir.7b01264
Langmuir 2017, 33, 9979−9987

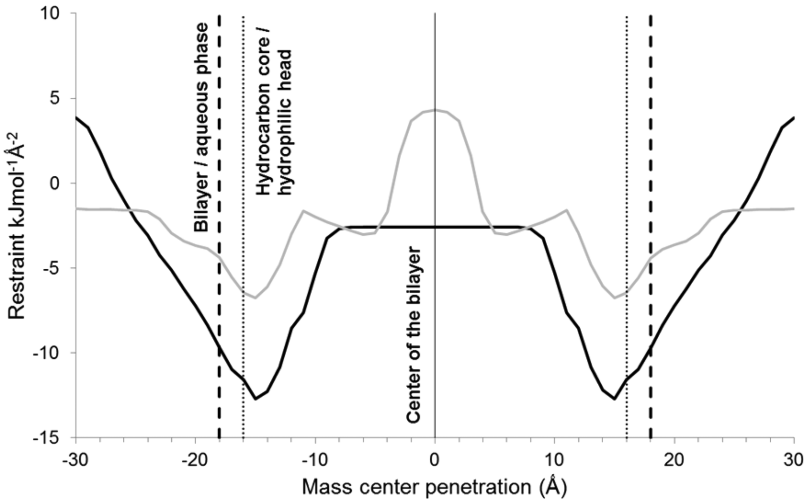

Figure 6. IMPALA plot of Alk-RL (black) and Ac-RL (gray) showing the energy restraints as a function of the mass center penetration.

The 3050−2800 cm^{-1} region of the pure PLPC (Figure 7A) spectra showed four bands (3010, 2955, 2924.5, and 2853.7

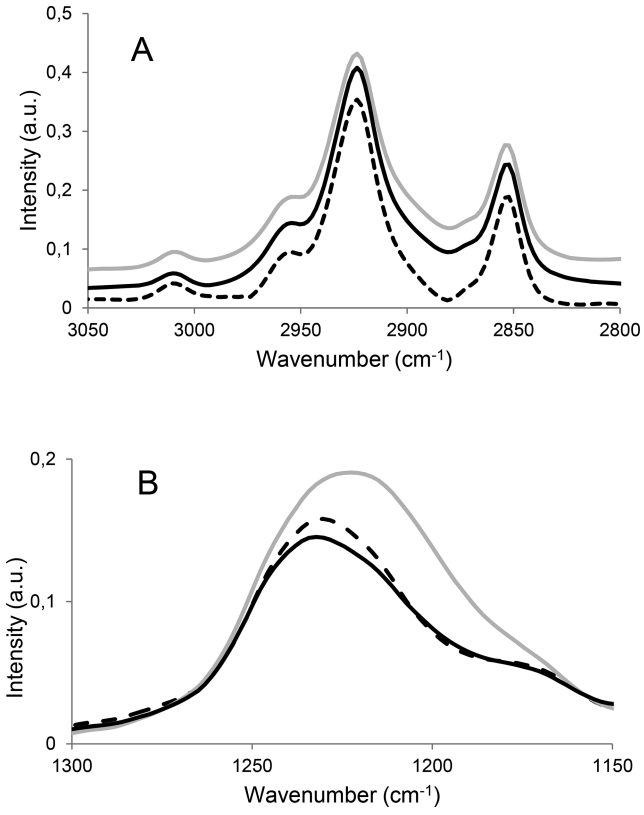

Figure 7. (A) 3050−2800 and (B) 1300−1150 cm^{-1} regions of the FTIR spectra of multilamellar vesicles composed of pure PLPC (discontinuous line), PLPC, and Alk-RL (black line) or PLPC and Ac-RL (gray line).

cm^{-1}) corresponding to the C═C, $-CH_3$, and asymmetric and symmetric vibrations of the $-CH_2$ groups, respectively, as already described.[35,36] The location of these bands is not affected by the presence of the synthetic RLs.

The 1300−1150 cm^{-1} region of the PLPC spectra showed the main band located at 1228 cm^{-1} that corresponds to the asymmetric vibration of P═O from the phosphate group (Figure 7B).[35] This band is affected in a different way in the presence of Alk-RL or Ac-RL. In the presence of Alk-RL, the changes were not significant, whereas the presence of Ac-RL leads to a wider phosphate band.

These changes indicate that P═O groups are in a more bonded state in the presence of Ac-RL and are in a less bounded state with Alk-RL. The changes occurring on the phosphate groups in the presence of Ac-RL could be due to the direct interaction between phosphate groups and Ac-RL molecules or to the modification of the lipid arrangement when Ac-RL was present within the system. Concerning Alk-RL, its presence likely modifies the lipid arrangement of the PLPC in which direct interaction with the phosphate groups is less likely because of the insignificant shift in the wavenumber of P═O absorbance.

For MLVs containing stigmasterol, the band at 2915 cm^{-1} was shifted to 2917 and 2919 cm^{-1} in the presence of Alk-RL and Ac-RL, respectively (Figure 8A and inset). This shift suggests an increase in the alkyl chain mobility,[37,38] i.e., a fluidizing effect of synthetic RLs on the bilayer,[39,40] with a greater effect for Ac-RL.

In the 1300−1150 cm^{-1} region of the FTIR spectra (Figure 8B), the similar position of the asymmetric stretching band of the P═O group indicates limited effects of the synthetic RLs on the polar head region of the phospholipids when stigmasterol is present.

Concerning the C═O ester groups of phospholipids, our findings show that they are involved within the interactions with both RLs. Indeed, we observe a slight but significant shift to higher wavenumbers in both cases (Figure S4). No difference is observed between Alk-RL and Ac-RL. Moreover, the presence of sterol seems not to affect the effects of RLs on C═O ester groups of phospholipids.

In silico approaches were further used to analyze the interactions of synthetic RLs with lipids at an atomic level. The assembly of each synthetic RL with PLPC and stigmasterol has been calculated by a docking method (Figure 9).[26]

Our calculations suggested that both RLs interact in a different way with the lipid molecules. Alk-RL forms a compact molecular assembly with PLPC (total area 562 $Å^2$), whereas Ac-RL-PLPC (total area 589 $Å^2$) assembly is more expanded. This is due to the carboxylic group of Ac-RL, which induces a different orientation toward the lipid molecules, decreasing the

DOI: 10.1021/acs.langmuir.7b01264
Langmuir 2017, 33, 9979−9987

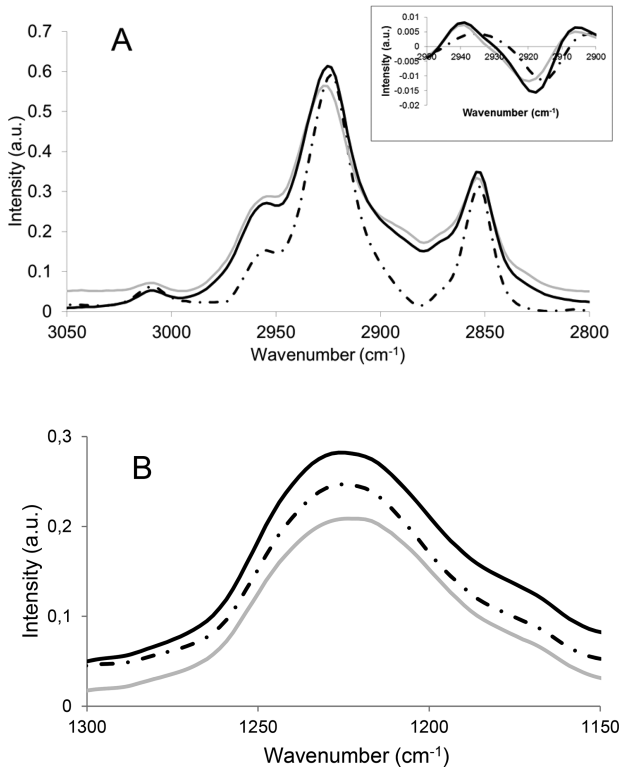

Figure 8. (A) 3050−2800 and (B) 1300−1150 cm^{-1} regions of the FTIR spectra of multilamellar vesicles composed of PLPC-stigmasterol (discontinuous line), PLPC-stigmasterol, Alk-RL (black line) or PLPC-stigmasterol, and Ac-RL (gray line). The inset of (A) shows the second derivative of the 2950−2900 cm^{-1} region of the FTIR spectrum.

hydrophobic interactions. For both molecules, the sugar residues and C═O ester groups of the synthetic RL were close to the phosphate group of phospholipids. The assembly with stigmasterol showed that the secondary alcohol group of the stigmasterol is at the level of the ester bound to the synthetic RLs, increasing the probability of hydrogen bond formation between both components.

DISCUSSION

Early Signaling Event Activation in Tobacco Cells after Their Challenge Using Synthetic RLs Depends on Their Chemical Structure. The production of ROS by plant cells could indicate a defensive state in association with the stimulation of defense gene expression and is characteristic of the successful recognition of external compounds by the plant cells.[22] Natural RLs produced by *Pseudomonas aeruginosa* have been shown to induce defense responses in grapevines, wheat, tobacco, and *Arabidopsis* cells.[3,41] In the early stages of the elicitation, this phenomenon is associated with extracellular ROS production in grapevines.[7] In addition, surfactin nC14 has been shown to induce a strong oxidative burst in tobacco cells and is able to induce a systemic resistance to fungal pathogens in several plant systems.[11,42] In this context, synthetic glycolipids were enzymatically synthesized using rhamnose as a polar headgroup with a fatty acid chain length of 14 carbons. Moreover, the syntheses of Ac-RL and of Alk-RL have been inspired from the carboxylic acid function present in natural RLs or the CH_3 present in natural RLs and surfactin. They were tested on tobacco cells to evaluate their capacity to induce extracellular ROS production. Both Ac-RL and Alk-RL induce significant ROS production, suggesting that synthetic RLs are perceived by plant cells and could be potential elicitor candidates. The response to Alk-RL was more important than that induced by Ac-RL treatment, and the ROS responses of both RLs are smaller than that of surfactin. The amphiphile structure of the molecules could therefore play a role in the perception by the plant cells with a higher potential of the alkyl-group-derived compounds.

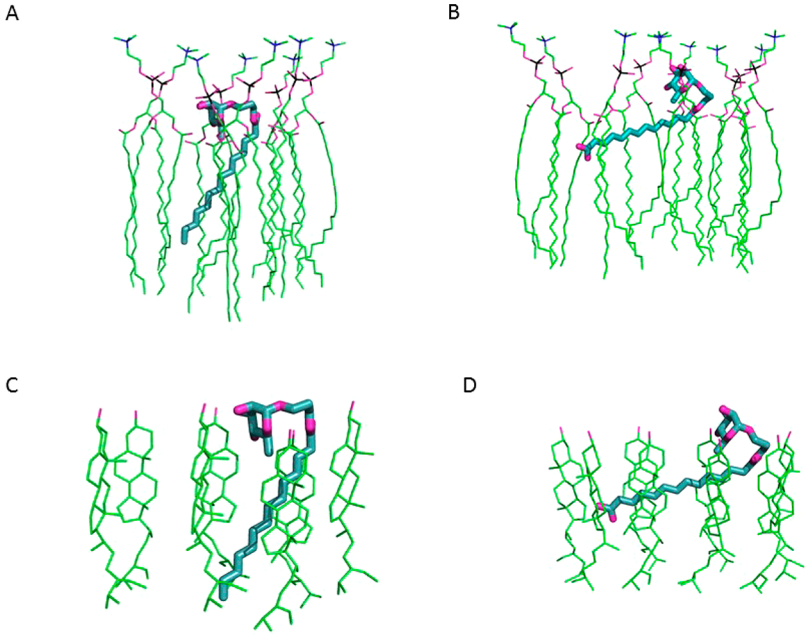

Figure 9. Molecular assemblies formed by Alk-RL-PLPC (A), Ac-RL-PLPC (B), Alk-RL-stigmasterol (C, and Ac-RL-stigmasterol (D). PLPC and stigmasterol are represented with lines, whereas synthetic RLs are represented with sticks; for the sake of clarity, hydrogens are not represented (carbons, green; oxygens, pink; nitrogens:, blue; phosphates, black).

DOI: 10.1021/acs.langmuir.7b01264
Langmuir 2017, 33, 9979−9987

Synthetic RLs Are Able to Interact with Membrane Lipids. Because some amphiphilic molecules such as surfactin were suggested to exert eliciting activity through interactions with the lipid phase of PPM,[11] we wondered if the structure/activity relationships observed for ROS production can be related to differences in the lipid interaction properties of both synthetic RLs. Therefore, the interactions of Alk-RL and Ac-RL with model membranes of plants were investigated at the molecular level by complementary biophysical tools. Both molecules are able to insert within monolayers constituted of PLPC, stigmasterol, and PLPC/stigmasterol, lipids that are representative of the PPM.[25,26] The maximal insertion pressure values were approximately 30 mN/m or higher, with a postulated value for the lateral pressure prevailing in biological membranes.[34] This result suggests that both synthetic RLs have the capacity to insert into natural membranes. The modeling approach is in agreement with this assumption because both molecules are able to insert into an implicit bilayer. Alk-RL seems to be more prone to interacting with bilayers compared to Ac-RL, in agreement with the adsorption measurements.

In the absence of stigmasterol within the unsaturated PC, the penetration power and lipid attraction are much higher for Alk-RL than for Ac-RL. Our FTIR data have shown that neither RL has an effect on the alkyl chains but does have a differential impact on the phosphate groups. Ac-RL strongly induces a more bonded state of the P═O groups, whereas Alk-RL gives rise to a less bonded state. The docking calculations also suggest direct interactions between PLPC phosphate groups and synthetic RLs. In the case of Ac-RL, its less appropriate binding to the lipids, as predicted by the modeling approach, could reduce the hydrophobic interactions, which can explain the absence of lipid attraction. The presence of the terminal carboxylic group can enhance the H-bond network at the level of the PC polar head and explain its higher impact on the phosphate groups. In contrast, the orientation of the acyl chain of Alk-RL parallel to the PL chains can favor its insertion by hydrophobic interaction within the fluid membrane without affecting the global alkyl chains' organization.

Surprisingly, the presence of stigmasterol within the PLPC matrix has a synergic effect on the insertion power and lipid attraction of both synthetic RLs, although it is reported in the literature[43] that stigmasterol reduces the membrane interface molecular mobility and, to a lesser extent, the molecular dynamics in the hydrophobic part of unsaturated PC bilayers. However, some studies[44,45] have also reported that cholesterol and plant sterols have the ability to induce lateral phase separation into a sterol-rich phase and a sterol-poor phase within an unsaturated PC matrix. This lateral phase separation creates phase boundaries that have been found to increase the membrane integration of CT-abscisic acid.[44] The same phenomenon can be suggested for the synthetic RLs, with a more attractive effect on the straight Alk-RL. If they preferentially insert into boundaries between the sterol-rich phase and the sterol-poor phase, then they are more likely to interact with stigmasterol than with PC molecules via H-bonds between the OH group of stigmasterol and the OH or ester groups of RLs, decreasing the effect on the PC phosphate groups compared to the pure PLPC membrane. However, in the PLPC/stigmasterol bilayers, both RLs show a fluidizing effect on the lipid alkyl chains, with a greater effect of Ac-RL. These results could be explained by a deeper position of the synthetic RLs within the plane of the PLPC/stigmasterol membrane in comparison to a pure PLPC membrane. In the case of Ac-RL, there could be a possible additional formation of a hydrogen bond between the terminal carboxylic moiety of Ac-RL and the OH group of stigmasterol. This could lead to an increase in the void volume between the lipid molecules, inducing a higher freedom of motion of the alkyl chains. In contrast, the predicted orientation of Alk-RL should not cause such an effect. However, the orientations of both RL molecules have to be validated experimentally to assess this assumption.

The organization of the membrane and the orientation of the RLs within the membrane then play key roles in the membrane interaction with RLs. More specifically, the interaction potency of the synthetic RLs with the boundary regions within the membrane could be related to the difference in the ROS activity observed between Alk-RL and Ac-RL.

The sole surface activity of the molecule cannot be correlated to the level of perception by the plant cells. Indeed, the surface activity of surfactin (γ_{CMC}= 27 mN/m[46]) is similar to that of Alk-RL (γ_{CAC} = 26 mN/m), whereas it shows a significantly higher ROS response. Moreover, this level of perception by the plant is not necessarily connected to the plant protection efficiency by the molecules. After the perception by the plant cells, other mechanisms far from being fully understood enter into play.

■ CONCLUDING REMARKS

In the literature, several studies have demonstrated that the perception of elicitors generally involves protein receptors at the membrane.[47−49] However, Henry et al. have suggested that surfactin, a lipopeptide having an amphiphilic structure and playing the role of an elicitor, is perceived by plants in a lipid-driven process at the plasma membrane level.[11] It was suggested that surfactin interaction with plasma membrane lipids could induce a lipid reorganization that triggers some recruitment and activation of key defense-related enzymes within particular microdomains of the plasma membrane.[11] The fact that both lipopeptides and synthetic RLs are amphiphilic molecules with one hydrocarbon chain led us to consider a similar mode of perception by plant cells, i.e., through a direct interaction with the lipid phase of the PPM. This hypothesis is supported by the fact that both Ac-RL and Alk-RL activate ROS production and that both compounds are inserting into plant-mimicking membranes. Our results also showed that both synthetic RLs have been perceived by cells in a dose-dependent manner and with a better perception for Alk-RL. These findings indicate that the interactions of Alk-RL and Ac-RL with model lipid membranes were different in terms of insertion, molecular interaction, and assembly formation and were dependent on the lipid composition of the model membranes. Taken together, our findings suggest that the perception of synthetic RLs could be related to a lipid-driven process. The role of a protein in the perception of the synthetic RLs cannot be ruled out at this stage, but this new way of eliciting is worth investigating. Alk-RL seems to be a better candidate than Ac-RL because of its greater ability to interact with membranes and its higher induction of ROS production by plant cells.

Further biological assays on the eliciting properties and deeper biophysical investigations into the lipid-interacting properties of these novel glycolipids should be the subject of further studies. Our study thus shows that a set of integrative biophysical approaches could serve as a predicting tool prior to more complex biological assays.

DOI: 10.1021/acs.langmuir.7b01264
Langmuir 2017, 33, 9979−9987

■ ASSOCIATED CONTENT

Supporting Information

The Supporting Information is available free of charge on the ACS Publications website at DOI: 10.1021/acs.langmuir.7b01264.

Viability test of tobacco root cells by Evans Blue in the presence and absence of Alk-RL. Determination of the critical aggregation concentration of synthetic rhamnolipids. Kinetics of the adsorption of Alk-RL and Ac-RL to a PLPC monolayer. FTIR spectra of multilamellar vesicles. PDF

■ AUTHOR INFORMATION

Corresponding Authors

*(M.N.N.) Tel: +32 81 62 22 55. E-mail: mn.nasir@ulg.ac.be.
*(M.D.) Tel: +32 81 62 26 38. Fax: +32 81 62 22 31. E-mail: magali.deleu@ulg.ac.be.

ORCID

Magali Deleu: 0000-0001-8255-2965

Notes

The authors declare no competing financial interest.

■ ACKNOWLEDGMENTS

We thank Mr. Pierre Monhonval for his technical assistance and Dr. Sébastien Mongrand for his fruitful discussions concerning plant membranes. We thank the Fonds National de la Recherche Scientifique (FRS-FNRS) (PDR grant T.1003.14), the Belgian Program on Interuniversity Attraction Poles initiated by the Federal Office for Scientific, Technical and Cultural Affairs (IAP P7/44 iPros), The University of Liège (Fonds Spéciaux de la Recherche, Action de Recherche Concertée-Project FIELD), EliDeRham project A2101-03 from the Region Champagne-Ardenne (France), and the Maelia project from Region Picardie (France) for financial support. M.D. and L.L. thank the FRS-FNRS for their positions as Senior Research Associates. J.-M.C. is supported by the IAP iPros project, and M.N.N. is supported by the ARC FIELD project.

■ REFERENCES

(1) Nott, K.; Richard, G.; Laurent, P.; Jérôme, C.; Blecker, C.; Wathelet, J.-P.; Paquot, M.; Deleu, M. Enzymatic Synthesis and Surface Properties of Novel Rhamnolipids. *Process Biochem.* **2013**, *48* (1), 133−143.

(2) Sanchez, M.; Teruel, J. A.; Espuny, M. J.; Marques, A.; Aranda, F. J.; Manresa, A.; Ortiz, A. Modulation of the Physical Properties of Dielaidoylphosphatidylethanolamine Membranes by a Dirhamnolipid Biosurfactant Produced by Pseudomonas Aeruginosa. *Chem. Phys. Lipids* **2006**, *142* (1−2), 118−127.

(3) Vatsa, P.; Sanchez, L.; Clement, C.; Baillieul, F.; Dorey, S. Rhamnolipid Biosurfactants as New Players in Animal and Plant Defense against Microbes. *Int. J. Mol. Sci.* **2010**, *11* (12), 5095−5108.

(4) Lang, S.; Wullbrandt, D. Rhamnose Lipids-Biosynthesis, Microbial Production and Application Potential. *Appl. Microbiol. Biotechnol.* **1999**, *51* (1), 22−32.

(5) Haferburg, D.; Hommel, R.; Kleber, H.-P.; Kluge, S.; Schuster, G.; Zschiegner, H.-J. Antiphytovirale Aktivität von Rhamnolipid Aus Pseudomonas Aeruginosa. *Acta Biotechnol.* **1987**, *7* (4), 353−356.

(6) Silipo, A.; Erbs, G.; Shinya, T.; Maxwell Dow, J. M.; Parrilli, M.; Lanzetta, R.; Shibuya, N.; Newman, M. A.; Molinaro, A. Glycoconjugates as Elicitors or Suppressors of Plant Innate Immunity. *Glycobiology* **2010**, *20*, 406−419.

(7) Ongena, M.; Jacques, P. Bacillus Lipopeptides: Versatile Weapons for Plant Disease Biocontrol. *Trends Microbiol.* **2008**, *16*, 115−125.

(8) Erbs, G.; Molinaro, A.; Dow, J. M.; Newman, M.-A. Lipopolysaccharides and Plant Innate Immunity. *Subcell. Biochem.* **2010**, *53*, 387−403.

(9) Cambiagno, D. A.; Lonez, C.; Ruysschaert, J.-M.; Alvarez, M. E. The Synthetic Cationic Lipid diC14 Activates a Sector of the Arabidopsis Defence Network Requiring Endogenous Signalling Components. *Mol. Plant Pathol.* **2015**, *16* (9), 963−972.

(10) Ranf, S.; Gisch, N.; Schäffer, M.; Illig, T.; Westphal, L.; Knirel, Y. A.; Sánchez-Carballo, P. M.; Zähringer, U.; Hückelhoven, R.; Lee, J.; et al. A Lectin S-Domain Receptor Kinase Mediates Lipopolysaccharide Sensing in Arabidopsis Thaliana. *Nat. Immunol.* **2015**, *16* (4), 426−433.

(11) Henry, G.; Deleu, M.; Jourdan, E.; Thonart, P.; Ongena, M. The Bacterial Lipopeptide Surfactin Targets the Lipid Fraction of the Plant Plasma Membrane to Trigger Immune-Related Defence Responses. *Cell. Microbiol.* **2011**, *13* (11), 1824−1837.

(12) Mulligan, C. N.; Wang, S. Remediation of a Heavy Metal-Contaminated Soil by a Rhamnolipid Foam. *Eng. Geol.* **2006**, *85* (1), 75−81.

(13) Pornsunthorntawee, O.; Wongpanit, P.; Rujiravanit, R. Rhamnolipid Biosurfactants: Production and Their Potential in Environmental Biotechnology. *Adv. Exp. Med. Biol.* **2010**, *672*, 211−221.

(14) Sekhon Randhawa, K. K.; Rahman, P. K. S. M. Rhamnolipid Biosurfactants-Past, Present, and Future Scenario of Global Market. *Front. Microbiol.* **2014**, *5*, 454.

(15) Maier, R. M.; Soberon-Chavez, G.; Soberón-Chávez, G. Pseudomonas Aeruginosa Rhamnolipids: Biosynthesis and Potential Applications. *Appl. Microbiol. Biotechnol.* **2000**, *54* (5), 625−633.

(16) Abdel-Mawgoud, A. M.; Lépine, F.; Déziel, E. *Appl. Microbiol. Biotechnol.* **2010**, *86*, 1323−1336.

(17) Banat, I. M.; Franzetti, A.; Gandolfi, I.; Bestetti, G.; Martinotti, M. G.; Fracchia, L.; Smyth, T. J.; Marchant, R. Microbial Biosurfactants Production, Applications and Future Potential. *Appl. Microbiol. Biotechnol.* **2010**, *87* (2), 427−444.

(18) Sanchez, L.; Courteaux, B.; Hubert, J.; Kauffmann, S.; Renault, J.-H.; Clément, C.; Baillieul, F.; Dorey, S. Rhamnolipids Elicit Defense Responses and Induce Disease Resistance against Biotrophic, Hemibiotrophic, and Necrotrophic Pathogens That Require Different Signaling Pathways in Arabidopsis and Highlight a Central Role for Salicylic Acid. *Plant Physiol.* **2012**, *160* (3), 1630−1641.

(19) Benschop, J. J.; Mohammed, S.; O'Flaherty, M.; Heck, A. J. R.; Slijper, M.; Menke, F. L. H. Quantitative Phosphoproteomics of Early Elicitor Signaling in Arabidopsis. *Mol. Cell. Proteomics* **2007**, *6* (7), 1198−1214.

(20) Finka, A.; Cuendet, A. F. H.; Maathuis, F. J. M.; Saidi, Y.; Goloubinoff, P. Plasma Membrane Cyclic Nucleotide Gated Calcium Channels Control Land Plant Thermal Sensing and Acquired Thermotolerance. *Plant Cell* **2012**, *24* (8), 3333−3348.

(21) Miller, G.; Schlauch, K.; Tam, R.; Cortes, D.; Torres, M. A.; Shulaev, V.; Dangl, J. L.; Mittler, R. The Plant NADPH Oxidase RBOHD Mediates Rapid Systemic Signaling in Response to Diverse Stimuli. *Sci. Signaling* **2009**, *2* (84), ra45.

(22) Torres, M. A. ROS in Biotic Interactions. *Physiol. Plant.* **2010**, *138*, 414−429.

(23) Zipfel, C.; Robatzek, S. Pathogen-Associated Molecular Pattern-Triggered Immunity: Veni, Vidi···? *Plant Physiol.* **2010**, *154* (2), 551−554.

(24) del Rio, L. A. ROS and RNS in Plant Physiology: An Overview. *J. Exp. Bot.* **2015**, *66* (10), 2827−2837.

(25) Murphy, A. S.; Peer, W.; Schulz, B. *The Plant Plasma Membrane*; Springer, 2010; Vol. *2010*.

(26) Deleu, M.; Crowet, J.-M.; Nasir, M. N.; Lins, L. Complementary Biophysical Tools to Investigate Lipid Specificity in the Interaction between Bioactive Molecules and the Plasma Membrane: A Review. *Biochim. Biophys. Acta, Biomembr.* **2014**, *1838* (12), 3171−3190.

DOI: 10.1021/acs.langmuir.7b01264
Langmuir 2017, 33, 9979−9987

(27) Razafindralambo, H.; Paquot, M.; Hbid, C.; Jacques, P.; Destain, J.; Thonart, P. Purification of Antifungal Lipopeptides by Reversed-Phase High-Performance Liquid Chromatography. *J. Chromatogr. A* **1993**, *639* (1), 81−85.
(28) Calvez, P.; Bussieres, S.; Eric, D.; Salesse, C.; Bussières, S.; Demers, É.; Salesse, C.; Bussieres, S.; Eric, D.; Salesse, C. Parameters Modulating the Maximum Insertion Pressure of Proteins and Peptides in Lipid Monolayers. *Biochimie* **2009**, *91* (6), 718−733.
(29) Calvez, P.; Demers, E.; Boisselier, E.; Salesse, C. Analysis of the Contribution of Saturated and Polyunsaturated Phospholipid Monolayers to the Binding of Proteins. *Langmuir* **2011**, *27* (4), 1373−1379.
(30) Lins, L.; Brasseur, R.; Malaisse, W. J. Conformational Analysis of Non-Sulfonylurea Hypoglycemic Agents of the Meglitinide Family. *Biochem. Pharmacol.* **1995**, *50* (11), 1879−1884.
(31) Ducarme, P.; Rahman, M.; Brasseur, R. IMPALA: A Simple Restraint Field to Simulate the Biological Membrane in Molecular Structure Studies. *Proteins: Struct., Funct., Genet.* **1998**, *30* (4), 357−371.
(32) Lins, L.; Brasseur, R. The Hydrophobic Effect in Protein Folding. *FASEB J.* **1995**, *9* (7), 535−540.
(33) Hädicke, A.; Blume, A. Binding of the cationic peptide $(KL)_4K$ to lipid monolayers at the air-water interface: effect of lipid headgroup charge, acyl chain length, and acyl chain saturation. *J. Phys. Chem. B* **2016**, *120*, 3880−3887.
(34) Marsh, D. Lateral Pressure in Membranes. *Biochim. Biophys. Acta, Rev. Biomembr.* **1996**, *1286* (3), 183−223.
(35) Ter-Minassian-Saraga, L.; Okamura, E.; Umemura, J.; Takenaka, T. Fourier Transform Infrared-Attenuated Total Reflection Spectroscopy of Hydration of Dimyristoylphosphatidylcholine Multibilayers. *Biochim. Biophys. Acta, Biomembr.* **1988**, *946* (2), 417−423.
(36) Arrondo, J. L. R.; Goñi, F. M. Infrared Studies of Protein-Induced Perturbation of Lipids in Lipoproteins and Membranes. *Chem. Phys. Lipids* **1998**, *96* (1−2), 53−68.
(37) Kodati, V. R. R.; Lafleur, M. Comparison between Orientational and Conformational Orders in Fluid Lipid Bilayers. *Biophys. J.* **1993**, *64* (1), 163−170.
(38) Pohle, W.; Gauger, D. R.; Dornberger, U.; Birch-Hirschfeld, E.; Selle, C.; Rupprecht, A.; Bohl, M. Hydration of Biological Molecules: Lipids versus Nucleic Acids. *Biopolymers* **2002**, *67* (6), 499−503.
(39) Tamm, L. K.; Tatulian, S. A. Infrared Spectroscopy of Proteins and Peptides in Lipid Bilayers. *Q. Rev. Biophys.* **1997**, *30* (4), 365−429.
(40) Pohle, W.; Selle, C.; Fritzsche, H.; Binder, H. Fourier Transform Infrared Spectroscopy as a Probe for the Study of the Hydration of Lipid Self-Assemblies. I. Methodology and General Phenomena. *Biospectroscopy* **1998**, *4*, 267−280.
(41) Varnier, A.-L.; Sanchez, L.; Vatsa, P.; Boudesocque, L.; Garcia-Brugger, A.; Rabenoelina, F.; Sorokin, A.; Jh, R.; Kauffmann, S.; Pugin, A.; et al. Bacterial Rhamnolipids Are Novel MAMPs Conferring Resistance to Botrytis Cinerea in Grapevine. *Plant, Cell Environ.* **2009**, *32* (2), 178−193.
(42) Raaijmakers, J. M.; De Bruijn, I.; Nybroe, O.; Ongena, M. Natural Functions of Lipopeptides from Bacillus and Pseudomonas: More than Surfactants and Antibiotics. *FEMS Microbiol. Rev.* **2010**, *34* (6), 1037−1062.
(43) Hellgren, L. I.; Sandelius, A. S. The Impact of Different Phytosterols on the Molecular Dynamics in the Hydrophobic/hydrophilic Interface Phosphatidylcholine−liposomes. *Physiol. Plant.* **2001**, *113*, 23−32.
(44) Katzer, M. *Biophysical Characterization of the Interaction between a Naturally Occuring Solute, the Plant Hormone Ct-Abscisic Acid, with Membranes*. Thesis, Indiana University, 2005.
(45) Ilangumaran, S.; Hoessli, D. C. Effects of Cholesterol Depletion by Cyclodextrin on the Sphingolipid Microdomains of the Plasma Membrane. *Biochem. J.* **1998**, *335* (2), 433−440.
(46) Yeh, M. S.; Wei, Y. H.; Chang, J. S. Enhanced Production of surfactin from *Bacillus subtilis* by addition of solid carriers. *Biotechnol. Prog.* **2005**, *21*, 1329−1334.
(47) Nimchuk, Z.; Eulgem, T.; Holt, B. F., III.; Dangl, J. L. Recognition and Response in the Plant Immune System. *Annu. Rev. Genet.* **2003**, *37*, 579−609.
(48) Ron, M.; Avni, A. The Receptor for the Fungal Elicitor Ethylene-Inducing Xylanase Is a Member of a Resistance-like Gene Family in Tomato. *Plant Cell* **2004**, *16* (6), 1604−1615.
(49) Felix, G.; Boller, T. Molecular Sensing of Bacteria in Plants: The Highly Conserved RNA-Binding Motif RNP-1 of Bacterial Cold Shock Proteins Is Recognized as an Elicitor Signal in Tobacco. *J. Biol. Chem.* **2003**, *278* (8), 6201−6208.

DOI: 10.1021/acs.langmuir.7b01264
Langmuir 2017, 33, 9979−9987